Pure appl. geophys. 159 (2002) 403–420
0033–4553/02/030403–18 $ 1.50 + 0.20/0

Pure and Applied Geophysics

Production-induced Normal Faulting in the Valhall and Ekofisk Oil Fields

MARK D. ZOBACK[1] and JENS C. ZINKE[1]

Abstract — *In situ* stress and pore pressure data from the Valhall and Ekofisk oil reservoirs indicate that at the onset of production in both fields an incipient state of normal faulting existed in the crest of the anticlinal structures. In contrast, on the flanks of the structures the initial least principal stress values indicate an almost isotropic state of stress. Oil production from both fields caused marked pore pressure reductions as well as poroelastic reductions of the least principal stress in both the crest and flanks of the two structures. We demonstrate that as a result of production-induced pore pressure and stress changes, normal faulting appears to have spread out from the crests of the structures on to the flanks. Further evidence of a normal faulting stress state at Valhall has been found using data from a passive seismic monitoring experiment. Numerous microearthquakes were recorded during a six week monitoring period that are located at the very top of the reservoir or in the shale caprock immediately above it. An inverse/composite focal plane mechanism of these microearthquakes is consistent with a normal faulting stress regime.

Key words: Production-induced normal faulting.

Introduction

In this study we utilize *in situ* stress and pore pressure data from the Valhall and the Ekofisk fields in the Central Graben area of the North Sea to investigate active faulting within the reservoirs and cap rocks. Active faulting in oil and gas reservoirs is of importance for a variety of reasons. From an engineering perspective, slip on active faults appears to be the cause of sheared casings of production wells in some fields (MAURY *et al.*, 1992) and, in others, shear slip on pre-existing faults and bedding planes appears to be a serious source of wellbore instability during drilling (e.g., WILLSON *et al.*, 1998). In many low permeability reservoirs, critically-stressed faults (i.e., faults that are active in the present stress field) contribute importantly to overall reservoir permeability (FINKBEINER *et al.*, 1998; DOHLAKIA *et al.*, 1998). In other cases, re-activation of reservoir bounding

[1] Department of Geophysics, Stanford University, Stanford, CA 94305, USA.
E-mail: zoback@pangea.stanford.edu.

faults can cause a loss of seal capacity and leakage to occur (e.g., WIPRUT and ZOBACK, 1999) and slip on active faults may control the vertical extent of oil and gas column that a fault-bounded reservoir can contain (e.g., FINKBEINER *et al.*, 2000).

There have been a number of case studies in which both fluid withdrawal and fluid injection appear to have induced active faulting in oil and gas reservoirs (review by GRASSO, 1992). Since the classic study of injection-induced earthquakes in the Rangely oil field in Colorado (RALEIGH *et al.*, 1972), induced faulting in oil and gas reservoirs is usually associated with pore pressure increases due to water-flooding or hydraulic fracturing. In this case increases in pore pressure causes slip along pre-existing faults by reduction of the effective normal stress on the fault plane. The Coulomb criterion can be written in terms of effective stresses as:

$$\tau = \mu(S_n - P_p) \tag{1}$$

where τ is the shear stress on the fault, S_n is the normal stress, P_p is the pore pressure and μ is the coefficient of friction (cf., JAEGER and COOK, 1971). Thus, by raising the pore pressure, the effective normal stress on pre-existing faults $(S_n - P_p)$ is reduced, making it possible for faulting to occur at a level of shear stress at which fault slip would normally not occur.

A second mechanism of induced faulting in the vicinity of oil and gas reservoirs is poroelastic stress changes in the medium surrounding a compacting reservoir (SEGALL, 1985, 1989, 1992). In this case, faulting is induced by the superposition of pre-existing stresses with the stresses caused by pore pressure decreases in the reservoir. Application of this theory to the Lacq field in France (FEIGNIER and GRASSO, 1990) demonstrates a reasonably good correlation between the theoretically expected location of seismicity and that observed as long as the pre-existing stress state in the vicinity of the reservoir is characterized by normal faulting with a vertical maximum principal stress (SEGALL *et al.*, 1994).

In the present study, we discuss another mechanism by which normal faulting within reservoirs might be induced by poroelastic stress changes. We demonstrate that the stress path associated with reservoir production in the Valhall and the Ekofisk fields is such that normal faulting is enhanced in the reservoirs by the poroelastic decreases in the least horizontal stress decreases accompanying production-induced pore pressure decline. While this may seem counterintuitive in light of the conventional relationship between pore pressure and failure expressed in equation (1), we demonstrate that this is theoretically correct in terms of the Coulomb criteria for the observed stress path in the two oil fields. By stress path we mean the change in horizontal stress magnitudes in the reservoir accompanying changes of pore pressure with production. Similar processes may be active in other oil and gas fields where normal faulting within reservoirs appears to have been induced by hydrocarbon production (cf., DOSER *et al.*, 1991).

The Valhall and Ekofisk Oil Fields

The Valhall Field and the Ekofisk Field are located within the Central Graben in the southern part of the Norwegian North Sea (see Fig. 1a). The Valhall structure trends NW-SE and is an elongated anticline along a structure locally known as the Lindesnes Ridge (MUNNS, 1985). The reservoir is at a depth of approximately 2400 m subsea and consists of two late Cretaceous oil bearing formations: the Tor formation and the underlaying Hod formation which are overlain by Paleocene and Eocene age shale cap rock (Fig. 1b). Both formations are soft chalk facies with a primary due to formation overpressure inhibiting mechanical compaction of the chalk. The discovery well was drilled in 1975 and the field went into production in October 1982.

The Ekofisk structure is an elongated anticlinal structure with a principal fold axis in an approximately, north-south direction (VAN DEN BARK and THOMAS, 1981). The reservoir depth is approximately 2900 m subsea and consists of two fractured chalk intervals: the Ekofisk formation (Danian) and the Tor formation (Maastrichtian). A relatively impermeable layer of argillaceous, siliceous, and cherty chalk separates the two oil bearing horizons. Despite the high porosity of the chalks (up to 51%), matrix permeability is low (about 1 md, THOMAS *et al*., 1987) and reservoir permeability ($\sim$150 md) appears to be controlled by an extensive natural fracture system (BROWN, 1987).

In the case of both of these fields, there has been significant concern about active faulting. There have been numerous occurrences of casing failures in both fields which have been interpreted as the result of shear along active faults. This is especially clear for casing failures in the shale caprock at Ekofisk (SCHWALL and DENNEY, 1994). Moreover, there is appreciable gas leakage through the shale cap rocks in both fields which may be exacerbated by flow through faults (MUNNS, 1985). Finally, it is well known that since Ekofisk went into production in 1971, appreciable sea-floor subsidence has occurred (e.g., NAGEL, 1998; RHETT, 1998), presumably due to compaction within the reservoir. Interestingly, even though full-field water flooding operations began at Ekofisk in 1987, subsidence has continued at a near constant rate of 38 cm/year. A limited amount of subsidence has occurred at Valhall (PATTILLO *et al*., 1998). If faulting is being exacerbated by oil production, slip on active faults may be contributing to the reservoir compaction causing sea floor subsidence.

Least Principal Stress and Pore Pressure Analysis

In this study we focus on the Valhall field because we had direct access to least principal stress and pore pressure data. We have been constrained to use only published data for the Ekofisk field. One important difference between the two fields is that there has been a major water flooding program at Ekofisk since 1987 to

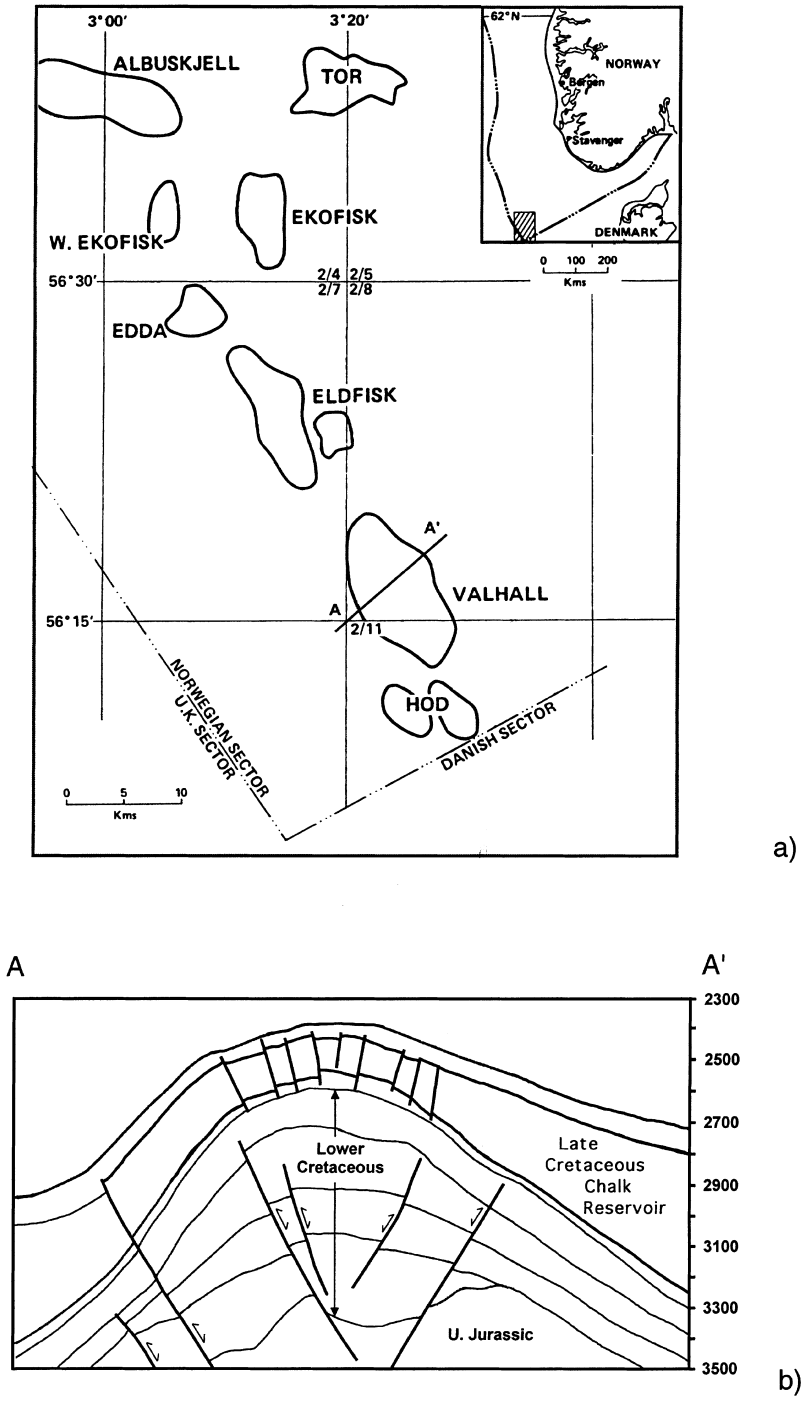

Figure 1
Location of the Valhall and Ekofisk oil fields are shown in a map of the southern Norwegian North Sea (a). A profile along line AA' illustrates the dome structure of the Valhall oil field (b).

maintain reservoir pressure and to attempt (unsuccessfully) to control subsidence. No water flooding has been carried out to date at Valhall. Because of this, we utilize stress and pressure data from Ekofisk acquired prior to the initiation of water flood operations. In fact, these data are similar to those at Valhall and lead to similar conclusions regarding induced faulting within the reservoir.

The data available from Valhall include conventional well logs, leak-off tests (LOTs) and minifracs to constrain the magnitude of the least principal stress, drillstem tests (DSTs) and remote formation tests (RTFs) to constrain pore pressure. Unfortunately, the original data from the pressure tests were not available to us. Data available from a passive seismic monitoring experiment consisted of microearthquake seismograms from six, three component seismometers deployed for a six week period in an observation well. These data are discussed below.

In Figure 2a we show a depth profile of all available pore pressure data at Valhall, and in Figure 2b we show all available estimates of the least principal stress. The vertical stress shown in Figure 2 was derived by integration of density logs. Leak-off tests (LOTs) and minifracs were used to constrain the least principal stress along with several formation integrity stresses (FITs). Remote formation test (RFT)

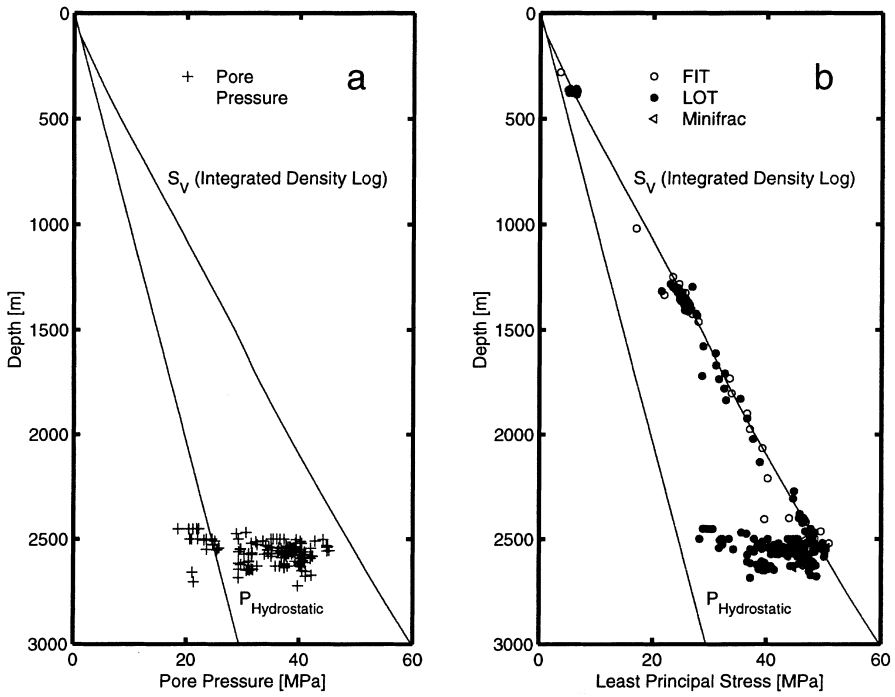

Figure 2
Depth profile of pore pressure (a) and least principal stress (b) at Valhall. LOT data appear to indicate that $S_3 \sim S_V$ in the overburden. In the reservoir, considerable scatter is seen in S_3 and in the pore pressure measurements, in part resulting from depletion in some parts of the reservoir.

data were principally used to constrain pore pressures. Pore pressure measurements are mainly limited to the reservoir ($\gtrsim$2400 m) and show considerable scatter, in part resulting from depletion in some parts of the reservoir. While the LOT data appear to indicate that $S_3 < S_v$ in the overburden ($\lesssim$2400 m), considerable scatter is seen in S_3 at the reservoir level. We interpret the scatter in S_3 values in the reservoir as being the result of production and accompanying poroelastic effects, as discussed below.

In Figure 3 we present the data from the reservoir section of the Valhall field (principally from the Tor formation) to evaluate the magnitude of the least principal stress with respect to pore pressure and position within the reservoir. To separate measurements with respect to their position in the crest or flank, we used the 2450 m depth contour on the top Tor structure map. By using colored symbols, we indicate the time that a given observation was made.

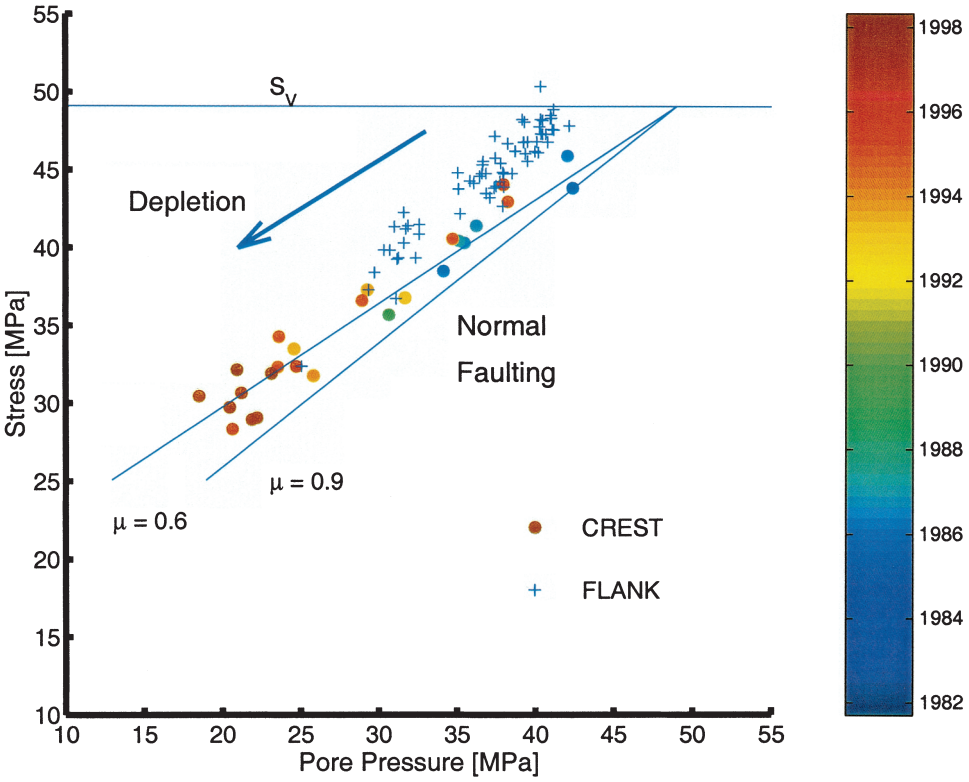

Figure 3
Least principal stresses versus pore pressure are shown for the Tor reservoir at Valhall. A horizontal line denotes the vertical stress S_V, and the inclined straight lines correspond to the Coulomb failure criterion for a coefficient of friction of 0.6 and 0.9 respectively. +'s denote values obtained for the flanks, and circles show values obtained for the crest. The color of the circles indicates the time that a given observation was made. As depletion progressed, pore pressure and stress dropped dramatically.

Several trends are apparent in these data. First, there is a clear reduction of pore pressure and S_3 with time that shows the overall effects of depletion. It is clear that both on the crest of the structure and on the flanks, pore pressures and least principal stresses in the reservoir were quite high in the early 1980s. As depletion occurred, pressure and stress dropped dramatically. On the crest of the structure, the change of the least principal stress with production ($\Delta S_3/\Delta P_p$) is about 0.7. The horizontal straight line in Figure 3 represents the vertical stress which is not expected to change with depletion for reservoirs which are laterally extensive with respect to their thickness (SEGALL and FITZGERALD, 1996). The inclined straight lines in Figure 4 correspond to the Coulomb failure condition for normal faulting utilizing coefficients of friction, μ, of 0.6–0.9, which are frequently measured in the laboratory for a wide variety of rocks (BYERLEE, 1978). The Coulomb failure condition is described by the following

$$(S_1 - P_p)/(S_3 - P_p) = ((\mu^2 + 1)^{1/2} + \mu)^2 \quad (2)$$

(JAEGER and COOK, 1971) where $S_1 = S_v$ and $S_3 = S_{h\min}$. TOWNEND and ZOBACK (2000) review numerous cases where the Coulomb criterion and laboratory-derived coefficients of friction accurately describe the *in situ* stress state.

Note that the data presented in Figure 3, under initial, undepleted conditions, show that the stress and pore pressure in the crest of the structure was in a normal faulting stress state, just as illustrated in the simplified sketch in Figure 4. As depletion occurred, the stress path, or the change of horizontal stress magnitudes due to reduction in the pore pressure, was such that the crest remained in a normal faulting stress state even though pore pressure was decreasing with time. Active normal faulting was the natural state and as production occurred, the stress path was such that normal faulting continued. The intermediate principal stress, S_2, in normal faulting areas corresponds to the maximum horizontal stress, $S_{H\max}$. It is expected that both horizontal stresses were affected more or less equally by depletion. While we have no direct estimates of $S_{H\max}$ magnitudes at Valhall, utilization of a variety of techniques indicates very little difference between the two horizontal stresses (KRISTIANSEN, 1998).

Figure 3 also demonstrates that stress magnitudes on the flanks of the Valhall structure were initially appreciably higher than on the crest. In fact, both pore pressures and least principal stress values were initially close to the overburden stress (well above the values observed in the crest) and certainly not consistent with normal faulting. In fact, if the maximum horizontal stress is intermediate in magnitude between the least horizontal stress and the vertical stress (as appears to be the case in the crest), the initial stress state on the flanks was almost isotropic. What is quite interesting, however, is that despite the nearly isotropic initial stress state, the stress path accompanying production on the flanks of the reservoir is such that once depletion has reduced pore pressure to about 30 MPa, a normal faulting stress state

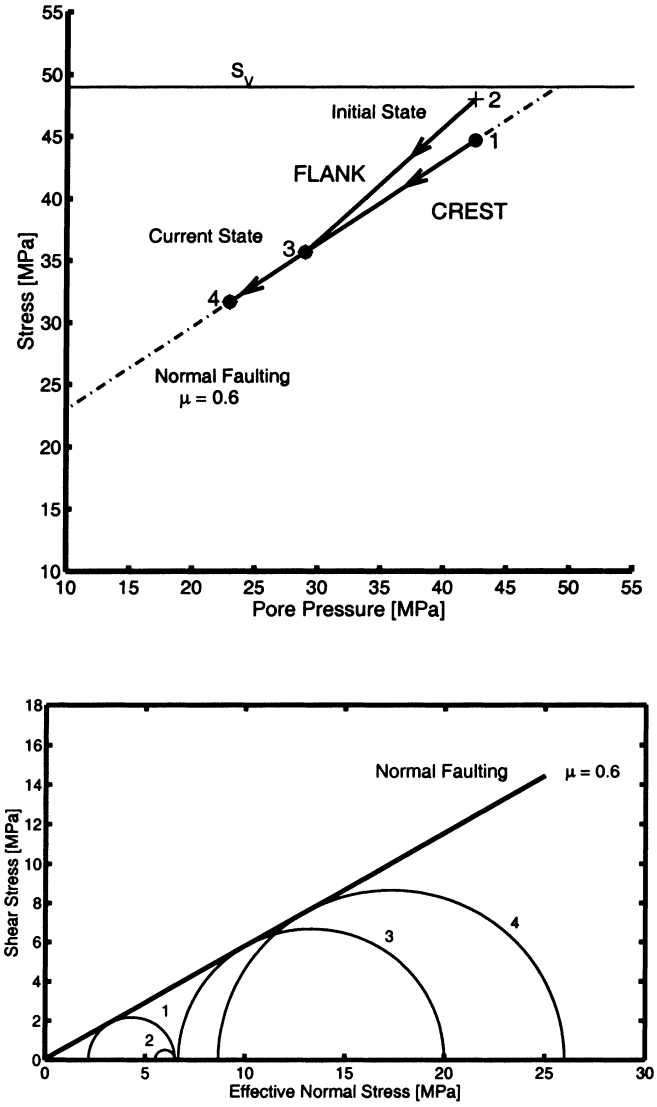

Figure 4

(a) Schematic relationship between initial stress states on the flank and crest of the Valhall structure (states 1 and 2, respectively) and their evolution (stress path) as the reservoir was depleted. A coefficient of friction of 0.6 was used to define a single failure line for simplicity. Note that the flank of the reservoir was not initially in a state of active normal faulting, the stress path was such that the normal faulting was induced by reservoir depletion. (b) Mohr-circle representation of the stress states shown in (a).

is encountered. Thus, depletion of the Tor formation appears to have induced normal faulting on the flanks of the reservoir. As normal faulting had already been occurring on the crest, it appears that it has spread outward from the crest of the structure onto the flanks as production and depletion have taken place.

The evolution of stress and pore pressure at Valhall are shown in a simplified sketch and accompanying Mohr diagrams in Figure 4. Initial stress conditions in the crest are illustrated by state 1 and evolve over time to states 3 and 4 as pore pressure is reduced and the least principal stress decreases due to poroelastic effects. Because the vertical stress does not change during depletion for laterally extensive reservoirs (SEGALL and FITZGERALD, 1996), the stress path is such that normal faulting is expected for each stress state (as illustrated by Mohr circles 1, 3 and 4).

The stress path and onset of faulting on the flanks of the Valhall reservoir are shown by states 2, 3 and 4 in Figure 4. The initial pore pressure and stress on the flanks (state 2) is certainly not consistent with normal faulting as the least principal stress is nearly equal to the vertical stress (note the extremely small Mohr circle). However, as pore pressure and stress change with production, the least horizontal effective stress increases slightly whereas the vertical effective stress increases considerably. Thus the stress path eventually intersects the normal faulting failure line (state 3) and with subsequent decreases in pore pressure, the least principal stress must decrease along this line because it cannot decrease more rapidly without exceeding the frictional strength of the reservoir (i.e., the Mohr circle cannot exceed the failure surface).

Poroelastic theory can be used to predict the magnitude of stress changes with depletion. For an isotropic, porous and elastic reservoir that is laterally extensive with respect to its thickness (i.e., a ratio of "breadth" to thickness greater than 20:1), the following expression (derived for an infinite, horizontal reservoir of finite thickness) is applicable (SEGALL and FITZGERALD, 1996).

$$\Delta S_h/\Delta P_p = \alpha\ (1-2v)/(1-v)\ , \tag{3}$$

where ΔS_h is the change in horizontal stress with a change in pore pressure (ΔP_p), v is Poisson's ratio and α is Biot's coefficient. $\alpha = 1 - K_b/K_g$, where K_b is the bulk modulus of the bulk rock and K_g is the bulk modulus of the mineral grains. It is clear from the observations in Figure 4 that on the flanks of the reservoir, $\Delta S_h/\Delta P_p$ is about 0.9. While we could attempt to use laboratory measurements of elastic modulii to compare this value with that expected value using equation (3), this is basically unnecessary. First, it is quite possible that the weak chalk reservoir is not deforming elastically. Second, because we have an observed stress path value of 0.88 on the flanks of the reservoir, we can consider it as being diagnostic of this reservoir under *in situ* conditions.

It is noteworthy that a nearly identical process is seen in the chalk reservoir of the Ekofisk field (Fig. 5), based on data from TEUFEL *et al.* (1991) which come from the time period prior to the initiation of water flooding operations. Because the Ekofisk structure has an oil column exceeding 300 m and we do not know the depths of the measurements reported by TEUFEL *et al.* (1991), which could come from a relatively large depth range, we have transformed pore pressure and least principal stresses into

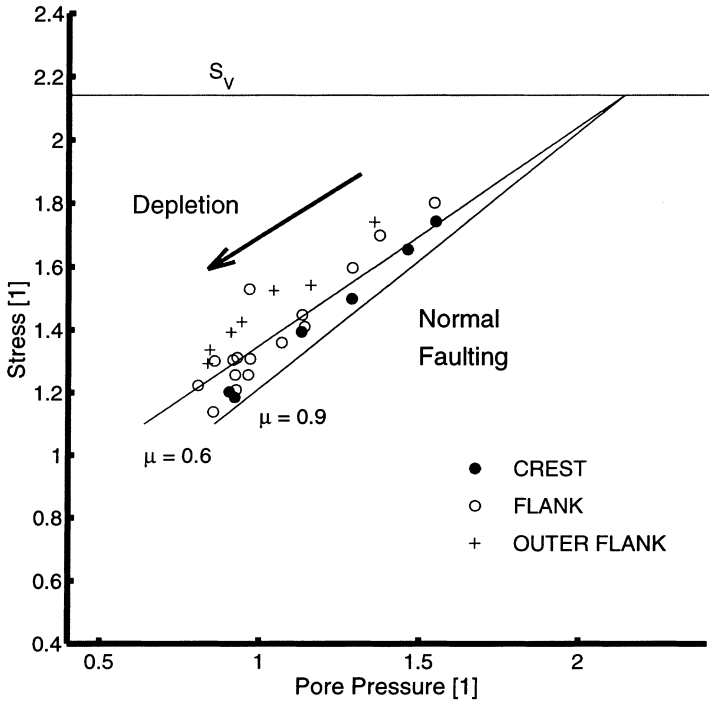

Figure 5
Least principal stresses versus pore pressure in terms of specific gravity are shown for the Ekofisk reservoir at Ekofisk (data from TEUFEL *et al.*, 1991). Filled circles, open circles, and crests denote values obtained for the crest, the flank, and the outer flank, respectively.

equivalent pressure gradients assuming an average depth of 2929 m, 3000 m, and 3075 m for the crest, flank, and outer flank of the structure, respectively. The vertical stress was obtained from integration density logs from several exploration wells.

Note in Figure 5 that the stress and pore pressure data from the Ekofisk reservoir demonstrate that just as at Valhall, under initial conditions, the crest of the structure was in a state of normal faulting but the flank and outer flank were not. Normal faulting would have been expected to continue as depletion and poroelastic stress changes occurred. As reservoir pressures decreased throughout, normal faulting was expected to spread out onto the flanks of the reservoir. The outer flank of the reservoir was almost in a state of normal faulting at the time of the last set of measurements.

TEUFEL *et al.* (1991) also discussed the data shown in Figure 5 in the context of faulting by relating the stress and pore pressure measurements to strength measurements made on Ekofisk core. However, our interpretation of incipient normal faulting in the crest of the structure and induced normal faulting on the flanks due to the poroelastic stress path expands upon their general interpretation.

Microearthquakes at Valhall and Ekofisk

Microseismic monitoring experiments were performed at both Valhall and Ekofisk. At Valhall, an array of six, three-component seismometers were deployed between June 1 and July 27, 1998 in a vertical section of one of the wells near the crest of the structure (Fig. 6). The seismic array was deployed about 300 m above the reservoir (Fig. 6). The spacing between the geophones was 20 m and the recorded seismic signals were digitized at 1 kHz. The locations of 328 microseismic events recorded during the ~7 week monitoring period are shown in Figure 6. Note that the majority of events occurred about 200 m to the west of monitoring well and that microearthquakes are occurring either at the very top of the reservoir or in the Paleocene shale cap rocks that overlay the Tor reservoir (MAXWELL, 2000).

To assess the state of stress in the Valhall cap rock associated with the microearthquakes, we could attempt to compute a focal mechanism for the events shown in Figure 6. However, because we have many earthquakes but effectively only a single recording site (i.e., the spacing of the sensors is much less than the path length), we computed a composite/inverse focal plane. To do this, we had to assume that the earthquakes were all occurring within a uniform stress field and all result from the same style of faulting (i.e., all would have the same focal plane mechanism had it been possible to analyze the events separately).

To obtain the inverse/composite focal mechanism, we positioned each microearthquake with respect to the focal sphere centered on each seismometer so that the ~300 events are assigned to different positions on the composite focal sphere. From the radiation patterns of a double-couple earthquake source (AKI and RICHARDS, 1980), it is known that the sign of the *P*-wave first motion is different in the four quadrants. In the focal plane mechanism shown in Figure 7, the filled symbols denote events with positive displacement, whereas open symbols denote events with negative displacement. Unfortunately, while the *P*-wave polarities suggest a normal fault mechanism (dilatations near the center of the focal sphere) the data are not sufficient to define the focal planes because of the limited distribution of microearthquakes.

In an attempt to overcome this limitation, we have also used *S*-to-*P* amplitude ratios because the position on the focal sphere where there is maximum *P*-wave amplitude (45° from the fault plane or auxiliary plane) coincides with the minimum of the *S*-wave amplitude. Similarly, we expect large S/P amplitude ratios (large symbols) along both the fault plane and the auxiliary plane, where the sign of the *P* wave changes from compressional to dilatational. We limited this analysis to waveforms with signal-to-noise ratios > 3. By combining the *P*-wave polarity and the S/P ratio data we define the focal mechanism shown in Figure 7. While there is considerable scatter in the mechanism due to the assumptions about the uniformity of the stress field and similarity of focal plane mechanisms that we have been required to make, the focal plane mechanism suggests normal faulting along NE-SW trending planes.

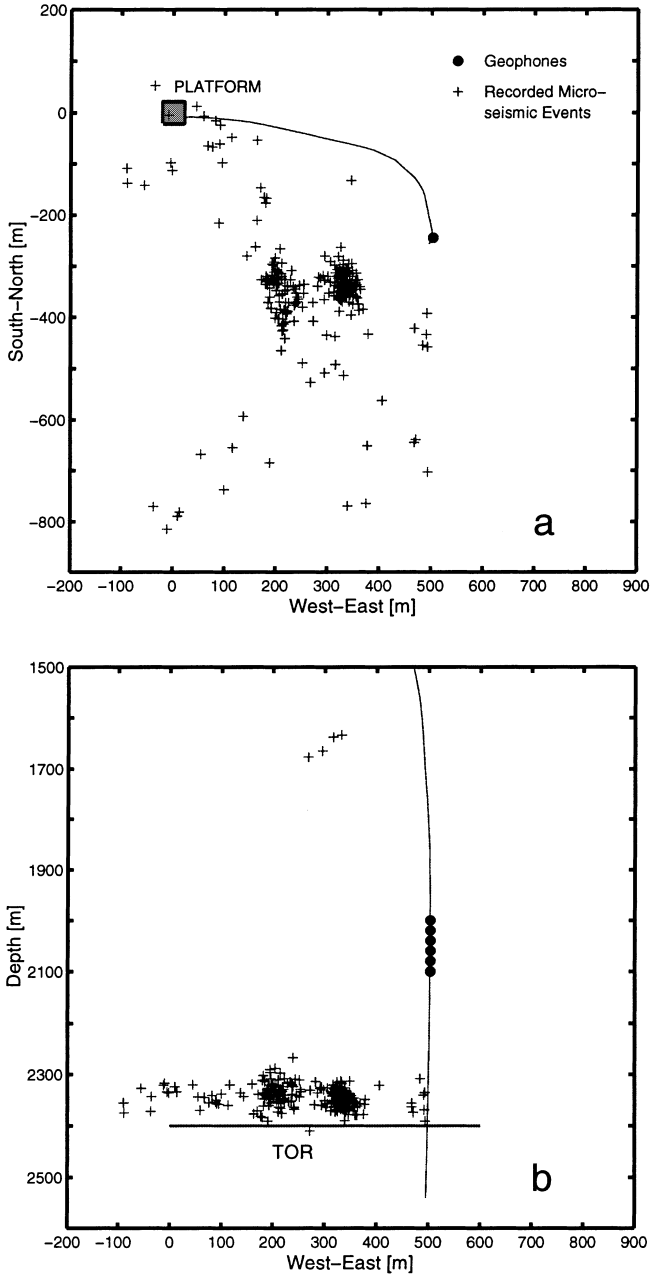

Figure 6
Well path with geophones and locations of the 328 at Valhall recorded microseismic events are shown in map view (a), and in a vertical west-east section (b). It is evident that the microseismic activity is concentrated in a narrow layer above the reservoir.

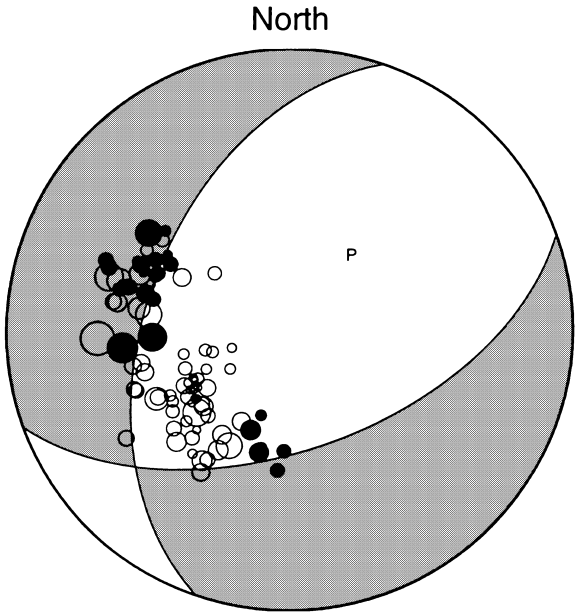

Figure 7
Inverse/composite focal mechanism for microearthquakes recorded at Valhall using the technique described in the text. The focal mechanism is an attempt to best fit both the polarity data (where open circles denote dilatational and filled circles denote compressional *P*-wave first motions) and *S*-to-*P* amplitude ratio (indicated by the size of the symbols). While there is considerable uncertainty in the focal plane mechanism, it is certainly suggestive of normal faulting.

Above a compacting reservoir we expect to observe an increase of horizontal compressive stresses and potentially, induced reverse faulting (see SEGALL, 1989). Because the earthquakes are normal faulting events, not thrust events, it suggests that the microearthquakes are not induced by the elastic stress changes due to compaction. Rather, they appear to be induced by normal faults propagating up into the cap rock from the reservoir. The least principal stress above the Valhall reservoir is either nearly isotropic or somewhat compressional because the vertical stress above the reservoir is equal to the least principal stress (Figs. 2, 3). While this might seem to suggest that production might induce reverse faulting there, the compressive stress perturbation above the reservoir is extremely small. As given by SEGALL and FITZGERALD (1996), immediately above a flat-lying ellipsoidal reservoir, the stress perturbation is given by

$$\Delta S_h/\Delta P_p = \alpha\{(1-2\nu)/(1-\nu)\}\{\pi/4\}\{A_3/A_1\} \ , \tag{4}$$

where A_3/A_1 is the ratio of the height of the reservoir, A_3, to its lateral extent, A_1. As A_3/A_1 is approximately 0.03 for Valhall, comparison of equations (3) and (4) demonstrates that the increase in horizontal stress with pore pressure changes due to production above the reservoir is only about 1% of the decrease in horizontal stress with pore pressure changes within it. In other words, the increase in horizontal

compressive stress would be ~0.2 MPa above the reservoir as opposed to ~20 MPa, within it. Thus, the only way in which reverse faulting could have been induced above the reservoir would have been if a reverse faulting stress regime existed there initially. The focal plane mechanism of the induced earthquakes indicates that this clearly was not the case. This suggests that the normal faulting above the reservoir was caused by the upward propagation of normal faults from within the reservoir.

It is important to note that the NE trend of the fault planes implied by the focal plane mechanism is not consistent with the NW trending fault plane orientations that appear in structure contour maps of the reservoir (MUNNS, 1985). One possible interpretation of this discrepancy is that the current state of stress in the reservoir is not the same as that which caused the movement on the NW trending faults. In fact, as the chalk is substantially thicker on the flanks of the reservoir (Fig. 1b) it seems clear that much of the deformation associated with the anticlinal structure was occurring as the chalk was being deposited in the late Cretaceous. In addition, the faults mapped within the reservoir cannot be mapped up into the Tertiary section (MUNNS, 1985). All of this suggests that the NW-trending faults in the reservoir are no longer seismically active. Unfortunately, no clear trend is seen in the distribution of the microearthquake events (Fig. 6a).

Microseismic recording was carried out at Ekofisk for 18 days in April, 1997 with the same 6-level seismometer system utilized at Valhall. In this case, the seismometers were deployed at the same depth as the reservoir in a well located in the crest of the structure (MAXWELL *et al.*, 1998). While the events near the wellbore could be located with relatively high accuracy, the depth and location of the events further away were more uncertain. In a detailed analysis of the microearthquake locations, MAXWELL *et al.* (1998) report that the majority of the events appear to occur in the upper part of the reservoir, apparently in low porosity, stiffer layers. They also argue that the well-located events cluster along discrete NE-trending lineations subparallel to mapped faults in the reservoir, obviously suggesting that water injection is triggering slip on these pre-existing faults. This may well be the case. However, as the pressure and stress data presented in Figure 5 show that the crest of the structure was in an incipient state of normal faulting even prior to the onset of water injection, this relationship could be somewhat more complex. It is interesting that the NE trend of the microseismic lineations and pre-existing faults in Ekofisk are subparallel to the fault planes implied by the focal mechanism derived for Valhall.

Discussion

Sheared Wells, Gas Leakage, Reservoir Permeability and Subsidence

The observations presented above have a variety of geomechanical implications. First, it is obvious that both the active normal faulting in the crest of the structures

and the induced faulting on the flanks may be responsible for some of the problems encountered with sheared well casings. It would be interesting to know if these problems "spread out" onto the flanks of the structures as the normal faulting stress state was reached. It is important to note that once the faulting process begins in part of the reservoir, water injection and pressure maintenance programs (such as implemented in Ekofisk) would not cause faulting to stop. In fact, once the pore pressure and least principal stress have "hit" the failure line (Figs. 3–5), faulting would be expected to continue unless water flooding actually reversed the pore pressure decline. Unfortunately, if the water injection caused local increases in pore pressure in the vicinity of faults it would likely trigger fault slip in terms of the conventional induced seismicity mechanism described at the beginning of this paper. This, of course, may also be directly relevant to compaction and subsidence at Ekofisk (c.f., NAGEL, 1998) as it is possible that some of the compaction and subsidence that has occurred is associated with slip on normal faults. One observation that may support this suggestion is that the initiation of a water injection and pressure maintenance program at Ekofisk did not cause subsidence to stop, or even slow down (NAGEL, 1998). Because of the arguments above, this is what would be expected in the case of slip on active faults. If reservoir compaction was the result of only the net increase in effective stress, the compaction should have stopped, or at least slowed down, once reservoir pressures stabilized.

With respect to reservoir permeability and gas leakage, active faulting in the reservoir is clearly a good news/bad news situation. The good news, of course, is that active faulting in the reservoirs is capable of increasing matrix permeability. BARTON *et al.* (1995), DHOLAKIA *et al.* (1998), CHANCHANI *et al.* (2001), and FINKBEINER *et al.* (1998) describe situations in which relatively small scale critically-stressed faults in the current stress field result in dramatic increases in reservoir permeability. It is quite interesting that despite the reservoir compaction accompanying depletion, reservoir productivity has remained steady, or has slightly increased, since production began (SULAK, 1991). In light of this observation, it is reasonable to assume that active shear faults may be enhancing the low matrix permeability (BROWN, 1987) and counteracting the permeability reductions expected to accompany compaction.

The bad news, of course, is that as there has been appreciable gas leakage through the shale cap rocks in both fields, which may have been exacerbated by enhanced fluid flow through faults propagating up into the cap rock from the reservoir. If the microseismicity is in the shale caprock at Valhall (Fig. 6), it is presumably due to the upward propagation of faults activated by fluid production in the reservoir. There also appears to be some faulting in the caprock at Ekofisk (MAXWELL *et al.*, 1998). Because of the water injection program at Ekofisk and the large strains accumulated over $\sim$20 years of production (as well as the uncertainties in determination of the exact depth of the microearthquakes which are distant from the observation well), it is difficult to interpret the microearthquakes at Ekofisk with confidence. Nonetheless, in light of our findings for both Ekofisk and Valhall, it is interesting to speculate if

there has been increased leakage caused by the initiation of faulting on the flanks of the reservoirs.

Conclusions

There are significant similarities in both the initial stress fields of the Valhall and Ekofisk fields and their evolution with time. In both fields, we found that under initial, undepleted conditions, the crest of the structures was in a state of active normal faulting. As depletion occurred, the stress path was such that the crest remained in a normal faulting stress state which appears to have spread outward to the flanks of the reservoirs. The locations of microseismic events reveal that normal faulting can be observed in and above the productive horizons. Whereas the normal faulting appears to be aseismic in the weak chalks of the reservoir, it is clearly seismic in the overburden. The significance of this as a possible mechanism responsible for problems with sheared well casings, reservoir permeability, cap rock integrity and subsidence is currently unknown.

Acknowledgements

We thank BP-Amoco for providing the data used in this study. Special thanks are due to L. Thomsen, M. Mueller, O. Barkved, T. G. Kristiansen, and P. G. Folstad from BP-Amoco for their assistance in data collection and constructive discussions. We thank S. C. Maxwell for constructive comments on the text. CSM Associates processed the seismic data of the passive seismic monitoring experiment and provided computed event locations. The views expressed in this paper are those of the authors and do not necessarily represent those of BP-Amoco or their co-ventures. Financial support for this project was provided by the Stanford Rock and Borehole Geophysics project.

References

Aki, K., and Richards, P. G., (*Quantitative Seismology*, *Theory and Methods*), vol. 1, (Freeman, San Fr ancisco, 1980), pp. 557.

Barton, C. A., Zoback, M.D., and Moos, D. (1995), *Fluid Flow Along Potentially Active Faults in Crystalline Rock*, Geology *23*, 683–686.

Byerlee, J. D. (1978), *Friction of Rock*, Pure appl. geophys. *116*, 615–626,

Brown, D. (1987), *The flow of water and displacement of hydrocarbons in fractured chalk reservoirs*. In *Fluid Flow in Sedimentary Basins and Aquifers* (eds. J. C. Goff and B. P. Williams) (Geological Society London) Special Publication *34*, 201–218.

Dholakia, S. K., Aydin, A., Pollard, D., and M. D. Zoback, (1998), *Development of Fault-controlled Hydrocarbon Migration Pathways in the Monterey Formation, California*, AAPG Bull. *82*, 1551–1574.

CHANCHANI, S. K., ZOBACK, M. D., and BARTON, C. (2000), *A Case Study of Hydrocarbon Transport Along Active Faults and Production-related Stress Changes in the Monterey Formation, California*, Geophys. Res. Lett., in press.

DOSER, D. I., BAKER, M. R., and MASON, D. B. (1991), *Seismicity in the War-Wink Gas Field, Delaware Basin, West Texas, and its Relationship to Petroleum Production*, Bull. Seismol. Soc. Am. *81*, 971–986.

FEIGNIER, B., and GRASSO, J. R. (1990), *Seismicity Induced by Gas Production: I. Correlation of Focal Mechanisms and Dome Structure*, Pure appl. geophys. *134*, 405–426.

FINKBEINER, T., BARTON, C. A., and ZOBACK, M. D. (1998), *Relationship Between in situ Stress, Fractures and Faults, and Fluid Flow in the Monterey Formation, Santa Maria Basin, California*, AAPG Bull. *81*, 1975–1999.

FINKBEINER, T., ZOBACK, M. D., Stump, B., and FLEMINGS, P. (2000), *Stress, Pore Pressure and Dynamically-constrained Hydrocarbon Column Heights in the South Eugene Island 330 Field, Gulf of Mexico*, AAPG Bull., (in press).

GRASSO, J. R. (1992), *Mechanics of Seismic Instabilities Induced by the Recovery of Hydrocarbons*, Pure appl. geophys. *139*, 507–533.

JAEGER, J. C., and COOK, N. G. W., *Fundamentals of Rock Mechanics* (Chapman and Hall, New York 1971).

KRISTIANSEN, G. (1998), *Geomechanical Characterization of the Overburden above the Compacting Chalk Reservoir at Valhall*, Eurock '98, SPE/ISRM Rock Mechanics in Petroleum Engineering, The Norwegian University of Science and Technology, Trondheim, Norway, 193–202.

MAXWELL, S. C., YOUNG, R. P., BOSSU, R., JUPE, A., and DANGERFIELD, J. (1998), *Microseismic Logging of the Ekofisk Reservoir*, Eurock '98, SPE/ISRM Rock Mechanics in Petroleum Engineering, The Norwegian University of Science and Technology, Trondheim, Norway, 387–393.

MAXWELL, S. C. (2000), *Comparison of Production-induced Microseismicity from Valhall and Ekofisk*, Paper presented at the Passive Seismic Method in E&P of Oil and Gas Workshop, 62nd EAGE Conference, May, 2000.

MAURY, V. M. R., GRASSO, J. R., and WITTLINGER, G. (1992), *Monitoring of Subsidence and Induced Seismicity in the Larq Gas Field* (*France*): *The Consequences on Gas Production and Field Operation*, Engineering Geology *32*, 123.

MUNNS, J. W. (1985), *The Valhall Field: A Geological Overview*, Marine and Petroleum Geology, *2*, 23–43.

NAGEL, N. B. (1998), *Ekofisk Field Overburden Modelling*, Eurock '98, SPE/ISRM Rock Mechanics in Petroleum Engineering, The Norwegian University of Science and Technology, Trondheim, Norway, 177–186.

PATTILLO, P. D., KRISTIANSEN, T. G., SUND, G. V., and KJELSTADLI, R. M. (1998), *Reservoir Compaction and Seafloor Subsidence at Valhall*, Eurock '98, SPE/ISRM Rock Mechanics in Petroleum Engineering, The Norwegian University of Science and Technology, Trondheim, Norway, 377–386.

RALEIGH, C. B., HEALY, J. H., and BREDEHOEFT, J. D. (1972), *An experiment in earthquake control at Rangely, Colorado*, Science *191*, 1230–1237.

RHETT, D. W. (1998), *Ekofisk Revisited: A New Model of Ekofisk Reservoir Geomechanical Behavior*, Eurock '98, SPE/ISRM Rock Mechanics in Petroleum Engineering, The Norwegian University of Science and Technology, Trondheim, Norway, 367–375.

SCHWALL, G. H., and DENNEY, C. A. (1994), *Subsidence Induced Casing Deformation Mechanisms in the Ekofisk Field*, Eurock '94, SPE/ISRM Rock Mechanics in Petroleum Engineering, Balkema, Delft, Netherlands, 507–515.

SEGALL, P. (1985), *Stress and Subsidence Resulting from Subsurface Fluid Withdrawal in the Epicentral Region of the 1983 Coalinga Earthquake*, J. Geophys. Res. *90*, 6801–6816.

SEGALL, P. (1989), *Earthquakes Triggered by Fluid Extraction*, Geology *17*, 942.

SEGALL, P. (1992), *Induced Stresses Due to Fluid Extraction from Axisymmetric Reservoirs*, Pure appl. geophys. *139*, 535.

SEGALL, P., GRASSO, J. R., and MOSSOP, A. (1994). *Poroelastic Stressing and Induced Seismicity Near the Lacq Gas Field, Southwestern France*, J. Geophys. Res. *99*, 15,423–15,438.

SEGALL, P., and FITZGERALD, S. D. (1996), *A note on Induced Stress Changes in Hydrocarbon and Geothermal Reservoirs*, Tectonophysics *289*, 117–128.

SULAK, R. M. (1991), *Ekofisk Field: The First 20 Years*, J. Petrol. Tech., 1265–1271.

TEUFEL, L. W., RHETT, D. W., and H. P. FARRELL, *Effect of reservoir depletion and pore pressure drawndown on in situ stress and deformation in the Ekofisk field, North Sea*. In *Rock mechanics as a Multidisciplinary Science* (ed. J. C. Roegiers) (Balkena, Rotterdam 1991), pp. 63–72.

THOMAS, L., DIXON, T., EVANS, C., and VIENOT, M. (1987), *Ekofisk Pilot Waterflood*, J. Petro. Tech. *39*, 221.

TOWNEND, J., and ZOBACK, M. D. (2000), *How Faulting Keeps the Crust Strong*, Geology *28*, 399–402.

WILLSON, S., LAST, N. C., ZOBACK, M. D., and MOOS, D. (1998), *Drilling in South America: A Wellbore Stability Approach for Complex Geologic Conditions*, SPE 53940, in 1999 SPE Latin American and Caribbean Petroleum Engineering Conference, Caracas, Venezuela *21–23* April, 1999.

WIPRUT, D., and ZOBACK, M. D. (1999), *Fault Reactivation and Fluid Flow Along a Previously Dormant Normal Fault in the Norwegian North Sea*, Geology *28*, 595–598.

(Received July 18, 2000, revised/accepted December 21, 2000)